StepReflect: Structured UI Transition Reflection for Mobile GUI Agents

Linqiang Guo[1], **Wei Liu**[1], **Li Gu**[1],
Yang Wang[1], **Tse-Hsun (Peter) Chen**[1]
[1]Concordia University
Montreal, Quebec, Canada
linqiang.guo@mail.concordia.ca, w_liu201@encs.concordia.ca,
li.gu@mail.concordia.ca, yang.wang@concordia.ca, peterc@encs.concordia.ca

arXiv:2608.05587v1 [cs.AI] 6 Aug 2026

Abstract

Autonomous mobile GUI agents require accurate action reflection for reliable long-horizon execution. Existing approaches rely on open-ended multimodal reasoning after each action, which is costly and poorly matched to the structured nature of GUI state transitions. We propose StepReflect, which formulates per-step GUI reflection as supervised structured prediction conditioned on explicit transition specifications and paired visual evidence. StepReflect is trained through a staged pipeline combining supervised fine-tuning, teacher–student distillation, and preference- and reward-based refinement. Offline, the resulting 8B model achieves 82.16% transition-level accuracy on AndroidWorld, exceeding zero-shot GPT-5.2 by 11.83 percentage points under the same structured input. Online, across M3A, Agent-SAMA, MAI-UI-8B, and Seed-2.0-Pro, StepReflect achieves higher task success in three of four agent configurations and remains within one successful task of the GPT-5.2 Reflection Agent in the fourth. It also reduces paid API charges relative to GPT-based reflection in all four configurations. These results establish StepReflect as a practical, locally deployable alternative to repeated frontier-model reflection for long-horizon mobile GUI agents.

1 Introduction

Autonomous mobile agents that operate graphical user interfaces (GUIs) are transforming how users interact with smartphones in the era of vision–language models (VLMs) (Yao et al. 2023; Wang et al. 2023). By interacting with apps through visual perception and low-level actions such as clicks, taps, and keystrokes, these agents can automate complex user workflows without relying on pre-defined scripts or platform-specific APIs. Recent advances in VLMs allow mobile GUI agents to perceive and act in increasingly complex environments (Zheng et al. 2024; Hong et al. 2024). Agents such as AppAgent (Zhang et al. 2023), Mobile-Agent-E (Wang et al. 2025), and CogAgent (Hong et al. 2024) demonstrate substantial progress in perception and high-level planning, while reliable long-horizon execution still depends on accurately assessing the outcome of each action. However, achieving reliable long-horizon execution remains challenging. Given a task, such as ordering food or booking a ride, a GUI agent must execute a sequence of GUI actions across multiple screens to achieve the desired outcome. A key challenge is action reflection. At each step, the agent must assess whether an executed action produced the expected interface transition. Over long trajectories, even small reflection errors can accumulate, allowing the agent to proceed from incorrect states and ultimately fail.

Existing GUI agents address this challenge through open-ended multimodal reasoning (Wang et al. 2025; Dai et al. 2025; Lu et al. 2026). At each step, agents query large VLMs to assess whether the current interface matches expectations. This treats reflection as a general reasoning problem, even though GUI interactions follow structured, predictable state transitions (Guo et al. 2026). Thus, reflection is complex and expensive, and does not scale well to long-horizon tasks that require reflection at every step. More broadly, this reflects a limitation recently identified for long-horizon agents: current systems remain fundamentally *reactive* (Chen 2026; Guo et al. 2026), lacking explicit structure, persistent state, and execution-grounded feedback in their reasoning. This mismatch between the structured nature of GUI transitions and the unstructured treatment of reflection motivates a reformulation of the problem. Rather than treating reflection as open-ended multimodal reasoning, we bring **state-awareness** directly into the reflection task: GUI action reflection is formulated as a **supervised structured prediction problem over UI state transitions**, where reflection reduces to determining whether an observed UI transition is consistent with the expected effect of an action under the current task context.

We propose **StepReflect**, a compact learned reflector that determines whether an executed GUI action produces the expected UI transition. It conditions paired BEFORE/AFTER visual evidence on an agent-provided transition specification and returns a structured reflection result. As a standalone module, StepReflect can be integrated into different agent frameworks without modifying their planning or action-generation policies.

We train StepReflect using two mobile agent benchmarks, SPA-Bench (Chen et al. 2025b) and Mobile-Eval-E (Wang et al. 2025), and evaluate it on AndroidWorld (Rawles et al. 2025) and MobileWorld (Quyu Kong et al. 2025) under both offline and online settings. In the *offline* setting, we evaluate reflection accuracy on 1,082 manually verified UI transitions, where StepReflect achieves 82.16% transition-level accuracy using Qwen3-VL-8B (Bai et al. 2025b), exceeding zero-shot GPT-4o (66.17%) and GPT-5.2 (70.33%) by 15.99 and 11.83 percentage points, respectively, under the same structured input. In the *online* setting, we integrate

StepReflect into four agent frameworks on AndroidWorld (M3A (Rawles et al. 2025), Agent-SAMA (Guo et al. 2026)) and MobileWorld (MAI-UI-8B (Hanzhang Zhou et al. 2025), Seed-2.0-Pro (ByteDance Seed 2026)). Across these integrations, StepReflect improves the reported end-to-end task success rate over the corresponding baseline on three frameworks (M3A, MAI-UI-8B, and Seed-2.0-Pro), while eliminating paid reflector-API calls through local inference. On Agent-SAMA, whose multi-agent FSM already contains a dedicated state-aware Reflection Agent, StepReflect achieves 55.56% task success compared with 58.33% for the original reflector, while reducing paid API cost. This pattern suggests that learned state-aware reflection is most beneficial when the host agent does not already contain a tightly coupled reflection mechanism, while offering a cost–accuracy trade-off when replacing one. Together, these results demonstrate that structured learned reflection can serve as a practical, locally deployable alternative to repeated frontier-model reflection across heterogeneous mobile agents.

Our contributions are summarized as follows:

- **Supervised structured reflection at the UI-transition level.** We formulate per-step GUI action reflection as supervised prediction over UI transitions. To the best of our knowledge, this is the first learned mobile-GUI reflection formulation that jointly uses explicit symbolic pre-/post-conditions, bounded trajectory, and BEFORE/AFTER visual evidence to assess an executed action.
- **StepReflect: a lightweight learned reflector transferable across agent frameworks.** StepReflect packages state-aware transition reflection into a single 8B VLM that outputs both a binary decision and a structured rationale. We demonstrate its integration into four heterogeneous agent frameworks without retraining their planning or action-generation policies.
- **A staged training pipeline calibrated for reflection's error asymmetry.** We design a staged optimization pipeline of supervised fine-tuning, teacher-student distillation, and preference- and reward-based refinement, explicitly targeting the asymmetric cost of false rejections in long-horizon execution and inducing both structured rationales and calibrated decision behavior.
- **Cross-benchmark and cross-framework empirical evaluation.** StepReflect reaches 82.16% transition-level accuracy on AndroidWorld, exceeding zero-shot GPT-5.2 by 11.83 percentage points under the same structured input. Online, it improves the reported task success rate on three of four evaluated frameworks. On Agent-SAMA, whose multi-agent FSM already provides framework-level state-awareness through a dedicated Reflection Agent and inter-agent coordination, StepReflect offers a favorable cost–accuracy trade-off, reducing paid API cost while remaining within 2.77 percentage points of the original reflector.

2 Related Work

Improving Efficiency in GUI Agents. Long-horizon GUI interaction makes inference cost and latency an important concern. Existing work reduces this overhead through prompt and agent-configuration optimization (Spiess et al. 2025; Zhou et al. 2025), caching and prefetching (Huang et al. 2025; Pan et al. 2025), and lightweight models for candidate-action selection (Dai et al. 2025). These methods primarily optimize planning, reasoning reuse, or pre-action selection, whereas StepReflect targets the repeated post-action decision of whether the realized UI transition matches the agent's expectation.

Domain-Specific Models for GUI Agents. Compact GUI models have been developed through trajectory generation and reinforcement learning (Ye et al. 2025; Lu et al. 2026), screenshot-based grounding (Cheng et al. 2024; Du et al. 2026), and pre-execution criticism (Wanyan et al. 2025). Agent-SAMA (Guo et al. 2026) is the closest framework-level precursor: it represents app execution as an FSM with predicted next-state descriptions and explicit pre-/post-conditions, and uses a prompted-MLLM Reflection Agent to compare these expectations with the observed screen. StepReflect retains this transition-level semantics but isolates reflection as a supervised learning problem, instantiates it in a dedicated 8B model, and connects it to heterogeneous host agents through framework-specific adapters.

Learned Reflection for Agents. Prior work studies reflection through prompting, process reward modeling, and knowledge distillation (Shinn et al. 2023; Madaan et al. 2023; Lightman et al. 2023; Hinton, Vinyals, and Dean 2015; Ho, Schmid, and Yun 2023; Hsieh et al. 2023; Qu et al. 2024). Digital-agent evaluators range from prompted trajectory and step-level assessment (Pan et al. 2024) to learned process reward models for action or task progress (Chae et al. 2025; Chen et al. 2025a). GUI-Reflection (Wu et al. 2025) and VisCritic (Qian 2026) learn action verification from post-action visual evidence, while Task-State Representation (Zheng et al. 2026) provides a training-free transition-aware wrapper. Unlike these approaches, StepReflect jointly conditions on an agent-provided transition specification—including action intent and explicit pre-/post-conditions—paired BEFORE/AFTER evidence, and a bounded same-subgoal history. It realizes this specification-conditioned post-action decision as a standalone learned module that returns both a reflection verdict and a structured rationale.

3 StepReflect

For GUI agents, a task τ is a natural-language goal that requires a sequence of GUI interactions (e.g., "*purchase some items using a specific app*"). We decompose τ into subgoals $\{g_k\}$, where each g_k describes an intermediate milestone toward completing the task. At step t, the agent acts to complete the current subgoal by executing an action a_t in a UI state s_t and reaches a new UI state s_{t+1}. We call (s_t, a_t, s_{t+1}) a UI transition. Transition reflection aims to determine whether the observed transition $s_t \rightarrow s_{t+1}$ is consistent with the intended effect of a_t under the current subgoal and task context.

3.1 Problem Definition

StepReflect addresses the problem of ***GUI transition reflection*** for autonomous mobile GUI agents. Figure 1 provides

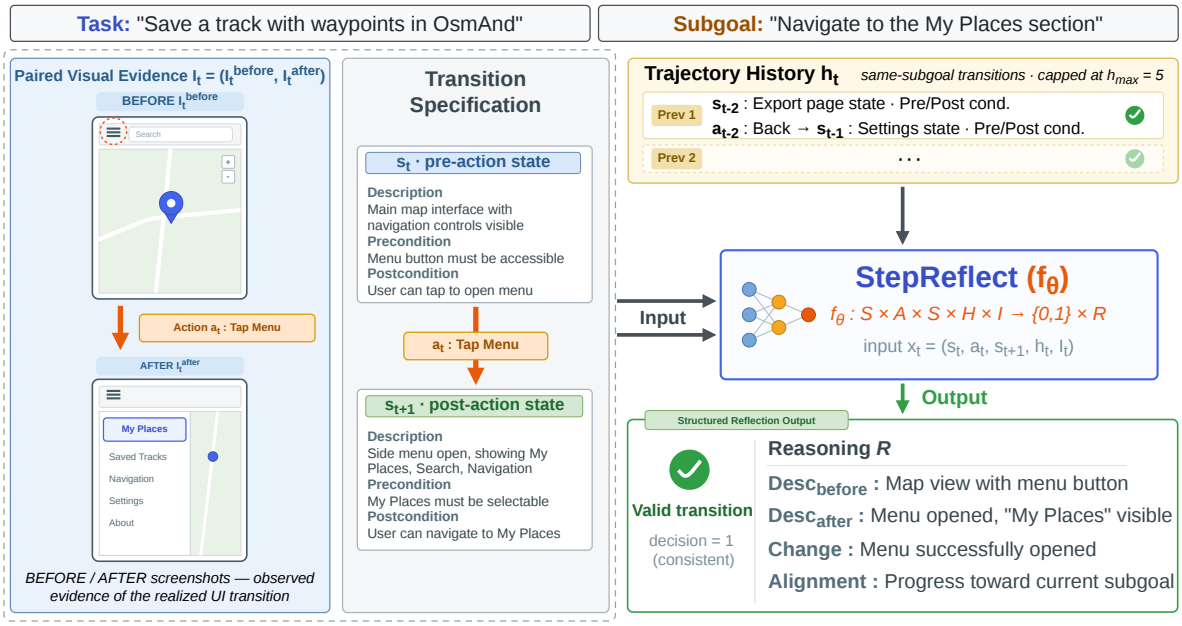

Figure 1: **Overview of StepReflect.** Given an agent-provided transition specification, bounded same-subgoal history, and paired BEFORE/AFTER screenshots, StepReflect predicts whether the executed action produced the intended UI transition and returns a structured rationale.

an illustration of StepReflect. After the GUI agent executes an action a_t, StepReflect observes the resulting UI state s_{t+1} and evaluates whether the transition from s_t to s_{t+1} is consistent with the *intended effect* of a_t, as specified by the agent's action description and current task state. StepReflect assesses consistency with the supplied expectation; it does not determine whether that expectation is itself correct.

Most existing GUI agents reflect on transitions by sending multimodal reasoning queries to large cloud-based VLMs, incurring high latency and cost that scale poorly with trajectory length. In contrast, we reformulate GUI reflection as a ***supervised, structured transition prediction problem***, avoiding open-ended reasoning and allowing efficient reflection with small- and medium-sized VLMs.

Formally, at step t, the reflector receives symbolic representations of the pre-action state $s_t \in \mathcal{S}$ and the post-action state $s_{t+1} \in \mathcal{S}$. These representations contain concise screen descriptions and the available pre-/post-condition fields. The reflector additionally receives the screenshot pair

$$I_t = \left(I_t^{\text{before}}, I_t^{\text{after}}\right) \in \mathcal{I},$$

which provides visual evidence of the realized transition.

Given the input tuple

$$x_t = (s_t, a_t, s_{t+1}, h_t, I_t),$$

where $h_t \in \mathcal{H}$ is a bounded history of recent transitions within the current subgoal, GUI transition reflection is defined as learning

$$f_\theta : \mathcal{S} \times \mathcal{A} \times \mathcal{S} \times \mathcal{H} \times \mathcal{I} \rightarrow \{0,1\} \times \mathcal{R}.$$

The binary output predicts whether the observed transition from s_t to s_{t+1} is consistent with the intended effect of a_t under the supplied task context, where 1 denotes a consistent transition and 0 denotes a mismatch. $\mathcal{R}$ is a natural-language rationale accompanying the decision and can be passed to the downstream agent as additional context.

3.2 GUI Action Transition Representation and Agent Integration

StepReflect performs GUI action reflection at the granularity of ***individual state transitions***. At each step t, we construct a reflection instance from the tuple (s_t, a_t, s_{t+1}, h_t), which represents the effect of a single action together with limited recent temporal context. This representation enables local reflection without requiring reasoning over entire execution trajectories.

StepReflect separates ***semantic expectations*** from ***observed evidence***. Semantic expectations are supplied by the host agent through the action intent and pre-/post-condition fields, which specify the expected state change. Observed evidence is supplied by the screen descriptions and paired screenshots associated with s_t and s_{t+1}, which represent the realized UI transition. StepReflect predicts whether the observed evidence is consistent with the supplied expectation. Because StepReflect does not generate the symbolic fields itself, errors in these upstream fields may propagate into its reflection decision.

To consider ***temporal context for reflection***, StepReflect incorporates a *subgoal-scoped* bounded trajectory history h_t. Concretely, h_t contains only those prior transitions that share the agent's current subgoal g_k, capped at $h_{\max}$=5:

$$h_t = \text{lastK}(\{(s_i, a_i, s_{i+1}) : g_i = g_k,\ i < t\},\ h_{\max}).$$

This design reflects the local, causal nature of GUI action reflection: transitions executed under earlier subgoals carry context that is rarely informative for verifying whether the current action aligns with its stated intent, and may mislead the reflector with unrelated state changes. The cap $h_{\max}=5$ is a context-safety bound rather than a tuned hyperparameter — in practice, the binding constraint on history length is the subgoal boundary itself, since most subgoals span only a few steps before the agent's stated intent shifts.

Finally, StepReflect is designed to ***integrate non-invasively with existing GUI agents***: a lightweight prompting interface maps each host agent's existing outputs onto the structured state representation defined in Section 3.1, without modifying the agent's policy, planning, or control logic.

3.3 Learning a GUI Transition Reflector

As shown in Figure 2, our fine-tuning pipeline comprises 3 stages that progressively equip the reflector with transition recognition and structured reflection behavior. We leverage Qwen2.5-VL (Bai et al. 2025a) (3B and 7B parameters) and Qwen3-VL (Bai et al. 2025b) (4B and 8B parameters) as base models. Both architectures support interleaved text and image inputs, making them suitable for multimodal transition reflection.

Stage 1: Supervised Fine-Tuning. We first apply supervised fine-tuning (SFT) to learn core GUI transition dynamics. Each training example instantiates the input tuple $x_t = (s_t, a_t, s_{t+1}, h_t, I_t)$ defined above, and the model is trained to output a structured JSON response containing a binary reflection decision and a natural-language explanation. This stage teaches the model to associate visual state changes, symbolic task abstractions, and action intent with correct transition outcomes, providing a stable optimization baseline.

Stage 2: Teacher–Student Distillation. To encourage more consistent rationale structure, we perform teacher–student distillation using GPT-5.2 (OpenAI 2025) as the teacher model. For each training instance, the teacher is prompted to describe the pre-action state, post-action state, observed UI changes, and their alignment with the current subgoal before producing a final reflection decision. The resulting rationale $\mathcal{R}$ can be passed to downstream agents as additional context. We then continue fine-tuning the SFT model on these distilled responses. Distillation produces substantially longer, template-structured outputs, but it does not consistently preserve standalone classification accuracy.

Stage 3: Preference and Reward-Based Refinement. Distilled variants produce longer, template-structured explanations, but some exhibit lower positive-class accuracy and therefore reject more valid transitions. We further refine StepReflect using preference-based and reward-based optimization to adjust this decision trade-off. We first apply Group Relative Policy Optimization (GRPO) (Guo et al. 2025), which samples multiple responses per input and optimizes them using a task-specific reward. To reflect the higher cost of false negatives in action reflection, we use an asymmetric reward design that penalizes incorrect rejections more strongly than incorrect acceptances. This encourages explicit reflection of observed outcomes rather than reliance on implicit assumptions. Specifically, correct "Yes" and "No" predictions receive rewards of +2.5 and +2.0, respectively, while false positives and false negatives incur penalties of -2.0 and -2.5.

In addition, we apply Direct Preference Optimization (DPO) (Rafailov et al. 2024) by constructing preference pairs through rejection sampling. For each input, we generate five candidate responses; instances where both correct and incorrect outputs are produced naturally yield preference pairs. DPO directly aligns the model toward reliable reflection behaviors without requiring an explicit reward model, complementing GRPO's reward-based optimization.

In summary, the three phases target different aspects of the reflection problem, from recognizing valid transitions to later refinement focusing on decision consistency.

3.4 Training Data

We construct training data for GUI transition reflection from execution trajectories generated by an interactive GUI agent on Mobile-Eval-E (Wang et al. 2025) and SPA-Bench (Chen et al. 2025b). These benchmarks cover 45 English cross-domain tasks across domains such as e-commerce, information management, and social media, spanning 40 apps. Each *interaction step* in a trajectory is treated as an independent training instance. At every step, we use the Reflection Agent design and prompting interface from AgentSAMA (Guo et al. 2026), while replacing its original GPT-4o-2024-11-20 backbone with GPT-5.2. This GPT-5.2-based re-instantiation produces an initial judgment of whether the executed action results in the intended UI change, using the BEFORE/AFTER screenshots, UI state, task context, and action metadata. The authors then audit and correct these initial judgments to obtain author-audited transition-level reflection labels. After filtering incomplete trajectories, the resulting training set contains 882 transition-level instances (517 positive, 58.6%; 365 negative, 41.4%). For evaluation, we use a **completely different** benchmark, AndroidWorld (Rawles et al. 2025).

4 Experiments

We evaluate StepReflect on AndroidWorld under two complementary settings to assess both its reflection capability in isolation and its effect when deployed within full agent execution loops. Following prior work (Ye et al. 2025), we consider **offline reflection** on fixed execution trajectories and **online reflection** through direct integration into existing agent frameworks.

4.1 Offline Reflection on AndroidWorld Trajectories

Setup. For offline evaluation, we use AndroidWorld (Rawles et al. 2025), which comprises 116 tasks involving one or more apps. Following the process described in Section 3.4, we construct a test set of 1,082 manually verified transition-level instances, including 613 positive samples (56.7%) and 469 negative samples (43.3%). Each transition is evaluated independently according to whether the observed UI change

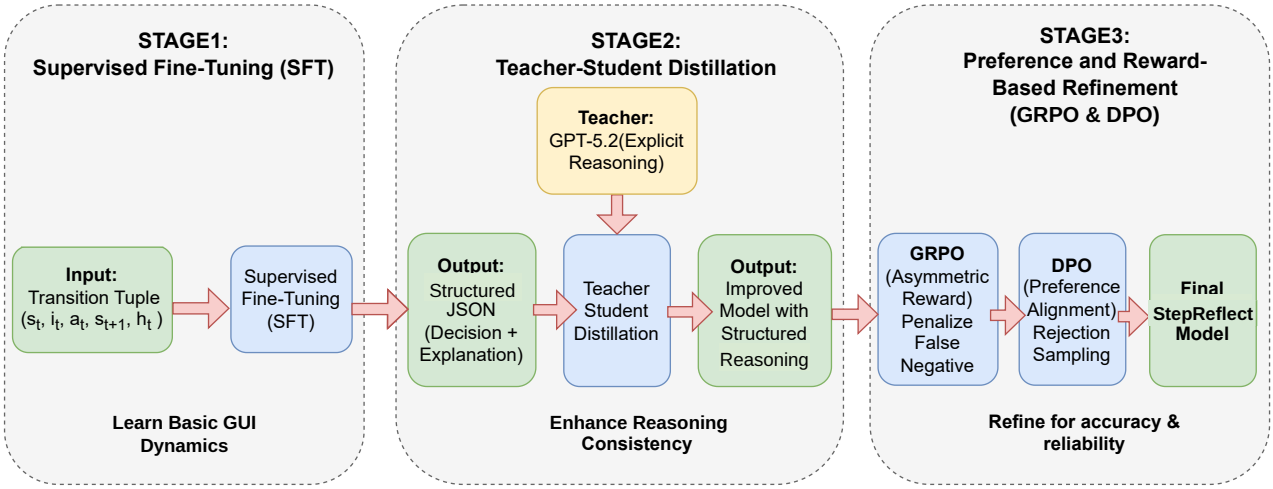

Figure 2: **StepReflect's three-stage training pipeline.** Supervised fine-tuning fits transition labels and the output schema; teacher–student distillation supplies structured rationale targets; and subsequent preference optimization refines the decision-error trade-off.

Model	Overall Acc.			Positive Acc.			Negative Acc.		
	Base	SFT	TS-Dis.	Base	SFT	TS-Dis.	Base	SFT	TS-Dis.
Qwen2.5-VL-3B	57.30	66.45	70.43	96.25	75.20	72.59	6.40	55.01	67.59
Qwen2.5-VL-7B	50.83	78.47	76.52	15.66	78.14	69.66	96.80	78.89	85.50
Qwen3-VL-4B	64.33	79.39	77.55	40.95	84.18	70.00	94.88	73.13	87.42
Qwen3-VL-8B	73.11	80.87	78.37	67.05	79.12	69.17	81.02	83.16	90.41
GPT-4o	66.17	–	–	51.88	–	–	84.86	–	–
GPT-5.2	70.33	–	–	51.39	–	–	95.10	–	–

Table 1: Offline transition accuracy on AndroidWorld. Results are computed on 1,082 transition-level instances, comprising 613 positive and 469 negative instances. We report overall accuracy and class-conditional positive and negative accuracy (%). All models receive the same structured input. Within each backbone, training is cumulative: Base → SFT → TS-Dis.

matches the intended effect of the executed action under the given task context.

We report transition-level success rate (SR), including *Overall SR*, *Positive SR* for correctly accepting expected UI transitions, and *Negative SR* for correctly rejecting unexpected or incorrect transitions. All models in Table 1, including GPT-4o and GPT-5.2, receive the same structured input—pre-/post-conditions, bounded history, BEFORE/AFTER screenshots, and action information. Therefore, the comparison isolates the effect of model choice and task-specific training rather than differences in the input representation.

Effect of base VLM choice and task-specific supervision. Table 1 shows that both SFT and TS-Dis. improve Overall SR over the corresponding base model across all four open-source backbones. For example, Qwen3-VL-8B improves from 73.11% to 80.87% Overall SR after SFT. Its Negative SR also rises from 81.02% to 83.16% after SFT and reaches 90.41% after TS-Dis., demonstrating stronger detection of unexpected or incorrect transitions. Moreover, the smaller Qwen3-VL-4B SFT model reaches 79.39% Overall SR, outperforming the larger Qwen3-VL-8B base model at 73.11%. This result shows that task-specific structured supervision can outweigh increased model scale.

Across comparable model sizes, Qwen3-VL consistently outperforms its Qwen2.5-VL counterpart. The base models also exhibit strong class-conditional biases in either direction, favoring either acceptance or rejection of UI transitions; task-specific supervision generally reduces these extreme behaviors. Under the identical structured input, the strongest SFT model, Qwen3-VL-8B, reaches 80.87% Overall SR, exceeding zero-shot GPT-5.2 by 10.54 percentage points and GPT-4o by 14.70 points.

Effect of reflection-objective refinement. Based on Table 1, we use Qwen3-VL-8B as the backbone and compare alternative post-SFT training objectives in Table 2. All variants share the same SFT initialization and differ in their subsequent distillation and GRPO/DPO refinement. GRPO achieves the highest Overall SR at 82.90%. DPO shifts the reflector toward rejecting invalid transitions, increasing Negative SR to 86.35% while reducing Positive SR to 77.32%.

The final StepReflect configuration reaches 82.16% Over-

Training Variant	Overall	Pos.	Neg.	Tokens
GRPO	**82.90**	83.20	82.52	65.9
DPO	81.24	77.32	86.35	68.2
TS-Dis. + GRPO	80.41	75.04	**87.42**	65.9
TS-Dis. + DPO	82.07	82.22	81.88	204.8
StepReflect	82.16	**86.79**	76.12	92.6

Table 2: Reflection-objective comparison on 1,082 AndroidWorld transitions using Qwen3-VL-8B. StepReflect is the final TS-Dis.→GRPO→DPO checkpoint; Tokens reports mean output length.

all SR, within 0.74 percentage points of the highest offline result, and achieves the highest Positive SR among all compared variants at 86.79%. This profile improves the model's ability to accept valid transitions and reduces unnecessary recovery in the downstream agent loop. Its average output length is 92.6 tokens. Overall, every refined variant exceeds zero-shot GPT-5.2 by at least 10.08 percentage points, while the final StepReflect exceeds it by 11.83 points under the same structured input.

4.2 Online End-to-End Evaluation with Integrated Reflection

Setup. We conduct online evaluation on two benchmarks and four agent frameworks: AndroidWorld (Rawles et al. 2025) with M3A (lightweight state-checking) and Agent-SAMA (Guo et al. 2026) (a dedicated Reflection Agent), and MobileWorld (Quyu Kong et al. 2025) with MAI-UI-8B (Hanzhang Zhou et al. 2025) and Seed-2.0-Pro (ByteDance Seed 2026) (both without built-in reflection).

For AndroidWorld, all conditions use the same fixed subset of 36 medium-difficulty tasks. This regime is most informative for evaluating an auxiliary reflector: simple tasks exhibit ceiling effects, whereas the hardest tasks are often dominated by upstream planning, grounding, or execution failures that post-action reflection alone cannot resolve. On M3A and Agent-SAMA, we compare their GPT-5.2 reflection components with SFT+GRPO and the final StepReflect. For MobileWorld, all conditions use the same 117 tasks. We add StepReflect as a reflection layer that consumes BEFORE/AFTER screenshots, state descriptions, action, and goal context, and appends a reflection hint to the next observation following a negative verdict. We compare no reflection, GPT-5.2 reflection, and StepReflect. The GPT-5.2 and StepReflect conditions receive identical inputs. When either reflector returns a negative verdict, its reflection feedback is appended to the next observation in the same way.

Effect of replacing built-in reflection components. Table 3 reports the online task success rates. On M3A, StepReflect achieves the highest result at 44.44%, outperforming the GPT-5.2 state summary by 5.55 percentage points and SFT+GRPO by 11.11 points. On Agent-SAMA, StepReflect reaches 55.56%, only one successful task (2.77 points) below its GPT-5.2 Reflection Agent, while outperforming SFT+GRPO by 5.56 points. Agent-SAMA's multi-agent FSM design already provides framework-level state-awareness through inter-agent coordination, leaving less room for a replacement reflector to alter end-to-end execution. Nevertheless, StepReflect remains competitive with its framework-specific frontier-model reflector while substantially reducing paid API charges.

Effect of adding reflection without pre-/post-conditions. The MobileWorld agents do not expose explicit pre-/post-conditions, providing a robustness test for description-only deployment inputs. On MAI-UI-8B, StepReflect achieves the highest task success rate at 29.91%, outperforming GPT-5.2 by 4.27 percentage points and the no-reflection condition by 8.54 points. On Seed-2.0-Pro, StepReflect reaches 41.88%, outperforming GPT-5.2 by 7.69 points while also remaining above the no-reflection condition by 0.85 points. Because both reflectors receive identical inputs and their feedback is incorporated into the next observation in the same way, the reflector model is the only changed reflection component. Across the four evaluated agent configurations, StepReflect achieves higher observed task success in three and remains within one successful task of the GPT-5.2 Reflection Agent in the fourth.

Effect of local deployment on paid API cost. Table 3 also shows that StepReflect reduces paid API charges across all four agent configurations. On M3A, it reduces the charge from $30.00 to $22.80, a saving of $7.20 (24.0%); on Agent-SAMA, it reduces the charge from $46.00 to $37.50, a saving of $8.50 (18.5%). On MAI-UI-8B, locally served StepReflect avoids the $3.16 GPT-5.2 reflector charge. On Seed-2.0-Pro, it reduces the charge from $22.21 with GPT-5.2 reflection to $14.60, while also remaining below the $15.86 no-reflection condition. Thus, StepReflect eliminates paid reflector API calls while preserving competitive or higher task success across heterogeneous agent frameworks.

Effect of reflector calibration. The paid-API cost difference alone does not explain StepReflect's stronger result relative to GPT-5.2 on Seed-2.0-Pro. GPT-5.2 issues negative verdicts at 19.3%, 8.0 percentage points higher than StepReflect's 11.3%, and triggers 42 early terminations compared with 19 for StepReflect. Our output analysis indicates that GPT-5.2 more frequently evaluates subgoal–action alignment, comparing the agent's stated coordinate intent with the executed action. In contrast, StepReflect is explicitly trained to judge the observed BEFORE-to-AFTER state change, allowing it to accept valid UI transitions even when execution differs from the agent's textual intent. The lower rejection rate and 23 fewer early terminations provide operational evidence that StepReflect's transition-specific calibration contributes to its higher end-to-end success rate.

4.3 Ablation Study

Setup. We conduct two controlled ablations on the same 1,082-transition AndroidWorld test set. All configurations use Qwen3-VL-8B with the same SFT and teacher–student-distillation initialization. The first ablation changes only the order of GRPO and DPO refinement. The second removes explicit pre-/post-conditions while retaining the final training pipeline.

Effect of refinement order. As shown in Table 4, applying

Agent	Reflector	Success (%)	Paid API (USD)
AndroidWorld (36 medium-difficulty tasks)			
M3A	GPT-5.2 summary	38.89	30.00
	SFT+GRPO	33.33	21.60
	StepReflect	44.44	22.80
Agent-SAMA	Reflection agent (GPT-5.2)	58.33	46.00
	SFT+GRPO	50.00	36.40
	StepReflect	55.56	37.50
MobileWorld (117 tasks)			
MAI-UI-8B	None	21.37	0.00
	GPT-5.2	25.64	3.16
	StepReflect	29.91	0.00
Seed-2.0-Pro	None	41.03	15.86
	GPT-5.2	34.19	22.21
	StepReflect	41.88	14.60

Table 3: Online task success rates and paid API charges. Paid API includes agent and hosted-reflector calls; local model serving and hardware costs are excluded.

GRPO before DPO yields higher Overall SR than the reverse order (82.16% vs. 80.41%) and substantially higher Positive SR (86.79% vs. 75.04%). Applying DPO before GRPO instead produces higher Negative SR (87.42% vs. 76.12%) but a more conservative reflector that more frequently rejects valid transitions. Such false rejections can trigger unnecessary recovery or replanning and propagate through long-horizon execution (Farid et al. 2022; Rawles et al. 2025; Wang et al. 2025). We therefore use GRPO followed by DPO in the final StepReflect configuration.

Effect of structured transition representation. In the description-only setting, each transition is represented as ⟨*from description, action, to description*⟩. The structured setting augments the transition with explicit pre- and post-conditions. As shown in Table 4, removing these structured signals reduces Overall SR by 4.25 percentage points (82.16%→77.91%) and Positive SR by 19.58 points (86.79%→67.21%). Although the description-only model reaches higher Negative SR (91.90% vs. 76.12%), its much lower Positive SR reveals a strong tendency to reject valid transitions. Explicit pre- and post-conditions reduce this conservative bias and produce both higher overall accuracy and a more balanced class-conditional profile. This result directly demonstrates the value of the proposed structured transition representation beyond natural-language state descriptions alone.

5 Limitations

Data and label scalability. Our supervision uses GPT-5.2-assisted reflection labels that are manually audited and corrected. This improves reliability over unverified model outputs but introduces human effort and limits scalability. Performance may also depend on the quality of the state descriptions and pre-/post-conditions supplied to the reflector. Larger-scale training would benefit from semi-automatic verification and active sampling of uncertain transitions.

Configuration	Overall SR (%)	Positive SR (%)	Negative SR (%)
Refinement order			
DPO → GRPO	80.41	75.04	87.42
GRPO → DPO (StepReflect)	82.16	86.79	76.12
Input representation			
Description-only	77.91	67.21	91.90
Structured (StepReflect)	82.16	86.79	76.12

Table 4: Ablations of refinement order and structured transition representation on 1,082 AndroidWorld transitions.

Evaluation and deployment scope. The AndroidWorld online evaluation uses 36 medium-difficulty tasks, targeting the regime where an auxiliary reflector can most directly affect execution; it does not represent full-benchmark performance. The online results also do not capture run-to-run agent, emulator, or API variation. Moreover, our non-invasive integration does not re-optimize the surrounding prompts or control logic, and the reported costs cover paid API charges but exclude local serving and hardware costs. Evaluating all 116 AndroidWorld tasks, repeated executions, and total deployment cost remains future work.

Cross-platform transfer. Validation focuses on mobile GUI agents. Extending the structured transition formulation to web or desktop environments would require adapting to different action spaces, layouts, interaction patterns, and state representations.

6 Conclusion

We presented StepReflect, a compact reflection module that formulates per-step GUI action reflection as supervised structured prediction over UI state transitions, separating it from open-ended multimodal reasoning. A staged training pipeline combining supervised fine-tuning, teacher–student distillation, GRPO, and DPO enables the 8B model to achieve 82.16% transition-level accuracy on AndroidWorld, exceeding zero-shot GPT-5.2 by 11.83 percentage points under the same structured input. Across four agent configurations on AndroidWorld and MobileWorld, StepReflect achieves higher observed task success in three and reduces paid API charges relative to the corresponding GPT-based component in all four. On Agent-SAMA, whose multi-agent FSM design already provides framework-level state-awareness, StepReflect remains within one successful task of the GPT-5.2 Reflection Agent while reducing paid API charges from $46.00 to $37.50. These results establish structured transition reflection as a reusable, locally deployable component for long-horizon GUI agents.

Appendix

This appendix provides the data, optimization, prompt, and evaluation details supporting the main paper. Sections are lettered according to the standard AAAI appendix convention.

A Data Construction and Evaluation Separation

A.1 Transition-level supervision

Each example represents one realized UI transition:

$$x_t = (s_t, a_t, s_{t+1}, h_t, I_t^{\text{before}}, I_t^{\text{after}}). \tag{1}$$

Here, s_t and s_{t+1} contain screen descriptions and available pre-/post-conditions, a_t is the executed action and stated intent, and h_t is bounded history. The target is a binary consistency judgment and a rationale. A positive label means that the observed UI change is consistent with the supplied transition expectation. It does not imply that the full task is complete or that the upstream expectation is globally optimal.

A.2 Training–evaluation separation

Training trajectories come from Mobile-Eval-E and SPA-Bench, covering 45 English cross-domain tasks and 40 apps. After filtering and audit, the collection contains 882 transitions: 517 positive (58.6%) and 365 negative (41.4%). Evaluation uses a separate AndroidWorld panel containing 1,082 manually verified transitions: 613 positive (56.7%) and 469 negative (43.3%). No AndroidWorld transition is used for SFT, teacher generation, DPO-pair construction, or GRPO updates.

A.3 Bounded history

History is scoped to the current subgoal and capped at $h_{\max} = 5$:

$$h_t = \text{lastK}\big(\{(s_i, a_i, s_{i+1}) : g_i = g_t,\ i < t\}, 5\big). \tag{2}$$

The subgoal boundary is applied before truncation. Transitions from a completed intent therefore cannot enter the current input even when recent.

A.4 Label audit and negative transitions

GPT-5.2 provides an initial judgment and rationale by comparing BEFORE/AFTER evidence with the stated action and expectation. Human audit corrects cases that confuse action intent, intermediate progress, visual evidence, or task completion. Incomplete records are filtered rather than assigned a guessed label.

Negative supervision combines audited failures with four implemented perturbations: no change, a past state from the same trajectory, a future state from the same trajectory, and a state from another task. These perturbations change transition pairing rather than image pixels. Held-out test labels are manually verified and are not produced by this procedure.

Table 5: Training configuration. Effective batch size includes gradient accumulation.

Stage	Epochs	Learning rate	Eff. batch
SFT	3	2×10^{-4}	8
TS-Dis.	3	1×10^{-4}	8
GRPO	1	1×10^{-6}	4
DPO	3	5×10^{-6}	16

B Training and Preference Optimization

We evaluate Qwen2.5-VL-3B/7B and Qwen3-VL-4B/8B. Adaptation uses 4-bit loading and LoRA with rank $r = 16$, scaling $\alpha = 16$, zero dropout, no bias, and seed 42. Adapters target the attention and feed-forward projection modules, and gradient checkpointing is enabled.

SFT and distillation use 8-bit AdamW, bfloat16 computation, cosine scheduling, and a 0.1 warmup ratio. Maximum sequence length is 8192 for SFT and distillation and 16384 for GRPO. GRPO samples four responses per prompt. DPO uses $\beta = 0.1$.

B.1 Asymmetric GRPO reward

The base classification reward is

$$R(\hat{y}, y) = \begin{cases} +2.5, & \hat{y} = \textsc{Yes},\ y = \textsc{Yes}, \\ +2.0, & \hat{y} = \textsc{No},\ y = \textsc{No}, \\ -2.0, & \hat{y} = \textsc{Yes},\ y = \textsc{No}, \\ -2.5, & \hat{y} = \textsc{No},\ y = \textsc{Yes}. \end{cases} \tag{3}$$

The stronger false-negative penalty reflects the downstream cost of rejecting a valid transition, which can trigger unnecessary recovery or termination. Smaller auxiliary adjustments reward valid JSON and evidence-bearing explanations; the label reward remains dominant.

B.2 Rejection-sampled DPO

Five candidates are sampled per input at temperature 0.8. An input is eligible only when sampling produces at least one correct and one incorrect verdict, ensuring that chosen and rejected responses share the same multimodal input. Of 647 candidate-generation inputs, 228 are eligible (162 expected Yes and 66 expected No), producing 488 preference pairs. Inputs for which all five candidates have the same correctness outcome produce no DPO pair.

C Prompt Templates and Runtime Contracts

Runtime values are represented by ⟨field⟩ placeholders. Repeated transition objects and history entries are data substitutions, not omitted instructions. No held-out AndroidWorld label, reward, or task result is supplied to a training or deployment prompt.

C.1 Structured SFT and offline-evaluation prompt

Listing 1: Structured transition-reflection prompt.

```
You are a mobile GUI reflector. Determine
    whether the
current state transition is valid, meaning
    whether it
aligns with the user's global task and
    current subgoal.

=== Global Task ===
<global_task>
=== Current Subgoal ===
<current_subgoal>
=== Current Transition ===
{
  "from_state": {
    "description": <before_description>,
    "precondition": <before_precondition>,
    "postcondition": <before_postcondition>
  },
  "action": {
    "type": <action_type>,
    "description": <action_description>,
    "arguments": <action_arguments>
  },
  "to_state": {
    "description": <after_description>,
    "precondition": <after_precondition>,
    "postcondition": <after_postcondition>
  }
}
=== Previous Steps (latest <N>) ===
<same_subgoal_transition_history>
=== Image Reference ===
<image_0>: Image BEFORE the action
<image_1>: Image AFTER the action
=== Question ===
Is this transition valid and aligned with
    the current
subgoal? Answer "Yes" or "No" and briefly
    explain why.
```

The supervised target follows the schema `{"answer":"Yes|No","reason":<evidence-based reason>}`.

C.2 Teacher rationale instruction

Teacher–student distillation appends the instruction below to prevent the teacher from requiring immediate completion of a multi-action subgoal.

Listing 2: Teacher rationale instruction.

```
IMPORTANT CLARIFICATION:
A subgoal may require multiple actions.
    Evaluate this
single realized transition, not completion
    of the entire
subgoal.

1. Describe the relevant BEFORE state.
2. Describe the relevant AFTER state.
3. Identify the observed UI change.
4. Compare the change with the intended
    local effect.
5. Decide whether the realized transition
    is consistent.
6. Return JSON:
   {"answer":"Yes|No","reason":"detailed
    reasoning"}

Do not answer "Yes" merely because the
    action would be a
plausible future step. Judge what actually
    occurred in the
BEFORE and AFTER evidence.
```

C.3 Refinement prompt reuse

GRPO and DPO introduce no new semantic user prompt. Both reuse Listing 1 under the Qwen chat template. GRPO stores the expected label outside model input for reward calculation. DPO constructs chosen and rejected completions under the identical text prompt and image pair. Thus, neither stage exposes the expected answer in the model input.

C.4 Description-only online adapter

M3A and the released Agent-SAMA adapter do not expose reliable pre-/post-condition fields at the adapter boundary. Their deployment template therefore retains task, subgoal, action, descriptions, history, and paired screenshots while omitting unavailable fields.

Listing 3: Description-only deployment prompt.

```
You are a mobile GUI reflector.
=== Global Task ===
<global_task>
=== Current Subgoal ===
<subgoal>
=== Current Transition ===
{
 "from_state":{"description":<
    before_description>},
 "action":{
   "type":<action_type>,
   "description":<action_description>,
   "arguments":<action_arguments>
 },
 "to_state":{"description":<
    after_description>}
}
=== Previous Steps (latest <N>) ===
<previous_steps>
<image_0>: Image BEFORE the action
<image_1>: Image AFTER the action
Is this transition valid and aligned with
    the current
subgoal? Answer "Yes" or "No" and briefly
    explain why.
```

For M3A, the subgoal slot is populated by the action model's reason string and the adapter passes the latest three truncated summaries. Agent-SAMA passes its current FSM subgoal and the latest five summary entries. A successful M3A verdict is injected as `SUCCESS: <reason>`; a failed verdict is injected as `FAILED: <reason>`. Agent-SAMA maps YES to outcome A and maps No to its host-compatible B/C failure subtype.

Table 6: Backbone comparison on the frozen 1,082-transition AndroidWorld panel (%). Training is cumulative within each backbone.

Model	Base	SFT	TS-Dis.
Overall accuracy			
Qwen2.5-3B	57.30	66.45	70.43
Qwen2.5-7B	50.83	78.47	76.52
Qwen3-4B	64.33	79.39	77.55
Qwen3-8B	73.11	80.87	78.37
GPT-4o	66.17	–	–
GPT-5.2	70.33	–	–
Positive accuracy			
Qwen2.5-3B	96.25	75.20	72.59
Qwen2.5-7B	15.66	78.14	69.66
Qwen3-4B	40.95	84.18	70.00
Qwen3-8B	67.05	79.12	69.17
GPT-4o	51.88	–	–
GPT-5.2	51.39	–	–
Negative accuracy			
Qwen2.5-3B	6.40	55.01	67.59
Qwen2.5-7B	96.80	78.89	85.50
Qwen3-4B	94.88	73.13	87.42
Qwen3-8B	81.02	83.16	90.41
GPT-4o	84.86	–	–
GPT-5.2	95.10	–	–

C.5 Runtime validation

The caller enforces the following contracts independently of prompt instructions:

- **SFT serialization:** both ordered images and required transition fields must be present; incomplete examples are removed.
- **Teacher generation:** the response must provide a recoverable verdict and rationale; audited labels remain authoritative.
- **GRPO:** invalid formatting receives a negative reward and is logged; the expected label is stored outside the prompt.
- **DPO:** chosen and rejected outputs must share the identical prompt and images; otherwise, no pair is created.
- **Online parsing:** image-load and response-parse failures are logged and do not silently become negative transition verdicts.

D Complete Offline Results

Let $P = 613$ and $N = 469$. We report

$$\mathrm{Acc} = \frac{TP + TN}{P + N}, \quad \mathrm{PosAcc} = \frac{TP}{P}, \quad \mathrm{NegAcc} = \frac{TN}{N}. \tag{4}$$

Class-conditional metrics expose acceptance/rejection bias that can be hidden by overall accuracy. Every model receives the same transition tuple and schema-based decoding.

Task-specific supervision improves overall accuracy relative to each base model while also reducing extreme class-conditional biases. For Qwen3-VL-8B, SFT raises overall accuracy from 73.11% to 80.87%. Final StepReflect reaches 82.16%, 11.83 points above zero-shot GPT-5.2 under the same structured input.

Table 7: Post-SFT objectives on Qwen3-VL-8B (%).

Variant	Overall	Pos.	Neg.	Tokens
GRPO	82.90	83.20	82.52	65.9
DPO	81.24	77.32	86.35	68.2
TS-Dis.+GRPO	80.41	75.04	87.42	65.9
TS-Dis.+DPO	82.07	82.22	81.88	204.8
StepReflect	82.16	86.79	76.12	92.6

Table 8: Controlled ablations on the same panel (%).

Configuration	Overall	Pos.	Neg.
DPO → GRPO	80.41	75.04	87.42
GRPO → DPO	82.16	86.79	76.12
Description-only	77.91	67.21	91.90
Structured	82.16	86.79	76.12

E Ablations and Online Integration

GRPO achieves the highest offline overall accuracy. The deployed checkpoint has the highest positive accuracy among the compared refinement variants, reducing unnecessary rejection of valid transitions while remaining within 0.74 points of the best overall score.

Structured inputs improve overall accuracy by 4.25 points and positive accuracy by 19.58 points relative to description-only inputs. Reversing the refinement order yields a more conservative model with higher negative but lower positive accuracy.

StepReflect runs after action execution and before the host's next planning step. It does not change policy weights, grounding, action space, emulator, or task evaluator. The online experiments use the fields exposed by each host; they are transfer evaluations rather than additional controlled ablations of pre-/post-conditions.

AndroidWorld uses the same fixed 36-task panel within each host; MobileWorld uses the same 117 tasks within each host comparison. These are within-host comparisons, not a cross-host ranking. StepReflect obtains the highest observed success in three of four configurations and is one successful task below the dedicated GPT-5.2 reflector on Agent-SAMA.

Table 9: AndroidWorld online results. Success is reported as successful tasks/36 (%); charge is USD.

Host	Reflection	Success	Charge
M3A	GPT-5.2 summary	14/36 (38.89)	30.00
	SFT+GRPO	12/36 (33.33)	21.60
	StepReflect	**16/36 (44.44)**	22.80
Agent-SAMA	GPT-5.2 reflector	**21/36 (58.33)**	46.00
	SFT+GRPO	18/36 (50.00)	36.40
	StepReflect	20/36 (55.56)	37.50

Table 10: MobileWorld online results. Success is reported as successful tasks/117 (%); charge is USD.

Host	Reflection	Success	Charge
MAI-UI-8B	None	25/117 (21.37)	0.00
	GPT-5.2	30/117 (25.64)	3.16
	StepReflect	**35/117 (29.91)**	0.00
Seed-2.0	None	48/117 (41.03)	15.86
	GPT-5.2	40/117 (34.19)	22.21
	StepReflect	**49/117 (41.88)**	14.60

References

Bai, S.; Chen, K.; Liu, X.; Wang, J.; Ge, W.; Song, S.; Dang, K.; Wang, P.; Wang, S.; Tang, J.; Zhong, H.; Zhu, Y.; Yang, M.; Li, Z.; Wan, J.; Wang, P.; Ding, W.; Fu, Z.; Xu, Y.; Ye, J.; Zhang, X.; Xie, T.; Cheng, Z.; Zhang, H.; Yang, Z.; Xu, H.; and Lin, J. 2025a. Qwen2.5-VL Technical Report. arXiv:2502.13923.

Bai, S.; et al. 2025b. Qwen3-VL Technical Report. arXiv:2511.21631.

ByteDance Seed. 2026. Seed2.0. https://seed.bytedance.com/en/seed2. Accessed: 2026-04-29.

Chae, H.; Kim, S.; Cho, J.; Kim, S.; et al. 2025. Web-Shepherd: Advancing PRMs for Reinforcing Web Agents. In *Advances in Neural Information Processing Systems (NeurIPS)*. Spotlight.

Chen, C.; Ji, K.; Zhong, H.; Zhu, M.; Li, A.; Gan, G.; Huang, Z.; Zou, C.; Liu, J.; Chen, J.; Chen, H.; and Shen, C. 2025a. GUI-Shepherd: Reliable Process Reward and Verification for Long-Sequence GUI Tasks. *arXiv preprint arXiv:2509.23738*.

Chen, J.; Yuen, D.; Xie, B.; Yang, Y.; Chen, G.; Wu, Z.; Yixing, L.; Zhou, X.; Liu, W.; Wang, S.; Zhou, K.; Shao, R.; Nie, L.; Wang, Y.; Hao, J.; Wang, J.; and Shao, K. 2025b. SPA-Bench: A Comprehensive Benchmark for SmartPhone Agent Evaluation. arXiv:2410.15164.

Chen, T.-H. 2026. Towards Structured, State-Aware, and Execution-Grounded Reasoning for Software Engineering Agents. arXiv:2602.04640.

Cheng, K.; Sun, Q.; Chu, Y.; Xu, F.; Li, Y.; Zhang, J.; and Wu, Z. 2024. SeeClick: Harnessing GUI Grounding for Advanced Visual GUI Agents. arXiv:2401.10935.

Dai, G.; Jiang, S.; Cao, T.; Li, Y.; Yang, Y.; Tan, R.; Li, M.; and Qiu, L. 2025. Advancing Mobile GUI Agents: A Verifier-Driven Approach to Practical Deployment. arXiv:2503.15937.

Du, Y.; Yan, Y.; Tang, F.; Lu, Z.; Zong, C.; Lu, W.; Jiang, S.; and Shen, Y. 2026. Test-Time Reinforcement Learning for GUI Grounding via Region Consistency. In *The Fortieth AAAI Conference on Artificial Intelligence*, AAAI'26.

Farid, A.; Veer, S.; Ivanovic, B.; Leung, K.; and Pavone, M. 2022. Task-Relevant Failure Detection for Trajectory Predictors in Autonomous Vehicles. In *6th Annual Conference on Robot Learning*, CoRL'22.

Guo, D.; et al. 2025. DeepSeek-R1 incentivizes reasoning in LLMs through reinforcement learning. *Nature*, 645(8081): 633–638.

Guo, L.; Liu, W.; Heng, Y. W.; Chen, T.-H.; and Wang, Y. 2026. Agent-SAMA: State-Aware Mobile Assistant. In *The Fortieth AAAI Conference on Artificial Intelligence*, AAAI'26.

Hanzhang Zhou, X. Z.; et al. 2025. MAI-UI Technical Report: Real-World Centric Foundation GUI Agents. arXiv:2512.22047.

Hinton, G.; Vinyals, O.; and Dean, J. 2015. Distilling the Knowledge in a Neural Network. arXiv:1503.02531.

Ho, N.; Schmid, L.; and Yun, S.-Y. 2023. Large Language Models Are Reasoning Teachers. arXiv:2212.10071.

Hong, W.; Wang, W.; Lv, Q.; Xu, J.; Yu, W.; Ji, J.; Wang, Y.; Wang, Z.; Zhang, Y.; Li, J.; Xu, B.; Dong, Y.; Ding, M.; and Tang, J. 2024. CogAgent: A Visual Language Model for GUI Agents. arXiv:2312.08914.

Hsieh, C.-Y.; Li, C.-L.; Yeh, C.-K.; Nakhost, H.; Fujii, Y.; Ratner, A.; Krishna, R.; Lee, C.-Y.; and Pfister, T. 2023. Distilling Step-by-Step! Outperforming Larger Language Models with Less Training Data and Smaller Model Sizes. arXiv:2305.02301.

Huang, K.-H.; Qiu, H.; Dai, Y.; Xiong, C.; and Wu, C.-S. 2025. GUI-KV: Efficient GUI Agents via KV Cache with Spatio-Temporal Awareness. arXiv:2510.00536.

Lightman, H.; Kosaraju, V.; Burda, Y.; Edwards, H.; Baker, B.; Lee, T.; Leike, J.; Schulman, J.; Sutskever, I.; and Cobbe, K. 2023. Let's Verify Step by Step. arXiv:2305.20050.

Lu, Z.; Chai, Y.; Guo, Y.; Yin, X.; Liu, L.; Wang, H.; Xiao, H.; Ren, S.; Xiong, G.; and Li, H. 2026. UI-R1: Enhancing Efficient Action Prediction of GUI Agents by Reinforcement Learning. In *The Fortieth AAAI Conference on Artificial Intelligence*, AAAI'26.

Madaan, A.; Tandon, N.; Gupta, P.; Hallinan, S.; Gao, L.; Wiegreffe, S.; Alon, U.; Dziri, N.; Prabhumoye, S.; Yang, Y.; Gupta, S.; Majumder, B. P.; Hermann, K.; Welleck, S.; Yazdanbakhsh, A.; and Clark, P. 2023. Self-Refine: Iterative Refinement with Self-Feedback. arXiv:2303.17651.

OpenAI. 2025. GPT-5.2 Model Documentation. https://platform.openai.com/docs/models/gpt-5.2. Accessed: 2026-01-19.

Pan, J.; Zhang, Y.; Tomlin, N.; Zhou, Y.; Levine, S.; and Suhr, A. 2024. Autonomous Evaluation and Refinement of Digital Agents. In *Conference on Language Modeling (COLM)*.

Pan, Z.; Patel, A.; Hu, Z.; Shen, Y.; Guan, Y.; Li, W.-L.; Qin, L.; Wang, Y.; and Ding, Y. 2025. KVFlow: Efficient Prefix Caching for Accelerating LLM-Based Multi-Agent Workflows. arXiv:2507.07400.

Qian, J. 2026. VisCritic: Visual State Comparison as Process Reward for GUI Agents. *arXiv preprint arXiv:2606.24525*.

Qu, Y.; Zhang, T.; Garg, N.; and Kumar, A. 2024. Recursive Introspection: Teaching Language Model Agents How to Self-Improve. arXiv:2407.18219.

Quyu Kong, X. Z.; et al. 2025. MobileWorld: Benchmarking Autonomous Mobile Agents in Agent-User Interactive and MCP-Augmented Environments. arXiv:2512.19432.

Rafailov, R.; Sharma, A.; Mitchell, E.; Ermon, S.; Manning, C. D.; and Finn, C. 2024. Direct Preference Optimization: Your Language Model is Secretly a Reward Model. arXiv:2305.18290.

Rawles, C.; Clinckemaillie, S.; Chang, Y.; Waltz, J.; Lau, G.; Fair, M.; Li, A.; Bishop, W.; Li, W.; Campbell-Ajala, F.; Toyama, D.; Berry, R.; Tyamagundlu, D.; Lillicrap, T.; and Riva, O. 2025. AndroidWorld: A Dynamic Benchmarking Environment for Autonomous Agents. arXiv:2405.14573.

Shinn, N.; Cassano, F.; Berman, E.; Gopinath, A.; Narasimhan, K.; and Yao, S. 2023. Reflexion: Language Agents with Verbal Reinforcement Learning. arXiv:2303.11366.

Spiess, C.; Vaziri, M.; Mandel, L.; and Hirzel, M. 2025. AutoPDL: Automatic Prompt Optimization for LLM Agents. arXiv:2504.04365.

Wang, G.; Xie, Y.; Jiang, Y.; Mandlekar, A.; Xiao, C.; Zhu, Y.; Fan, L.; and Anandkumar, A. 2023. Voyager: An Open-Ended Embodied Agent with Large Language Models. arXiv:2305.16291.

Wang, Z.; Xu, H.; Wang, J.; Zhang, X.; Yan, M.; Zhang, J.; Huang, F.; and Ji, H. 2025. Mobile-Agent-E: Self-Evolving Mobile Assistant for Complex Tasks. arXiv:2501.11733.

Wanyan, Y.; Zhang, X.; Xu, H.; Liu, H.; Wang, J.; Ye, J.; Kou, Y.; Yan, M.; Huang, F.; Yang, X.; Dong, W.; and Xu, C. 2025. Look Before You Leap: A GUI-Critic-R1 Model for Pre-Operative Error Diagnosis in GUI Automation. arXiv:2506.04614.

Wu, P.; Ma, S.; Wang, B.; Yu, J.; Lu, L.; and Liu, Z. 2025. GUI-Reflection: Empowering Multimodal GUI Models with Self-Reflection Behavior. In *Advances in Neural Information Processing Systems*.

Yao, S.; Zhao, J.; Yu, D.; Du, N.; Shafran, I.; Narasimhan, K.; and Cao, Y. 2023. ReAct: Synergizing Reasoning and Acting in Language Models. arXiv:2210.03629.

Ye, J.; Zhang, X.; Xu, H.; Liu, H.; Wang, J.; Zhu, Z.; Zheng, Z.; Gao, F.; Cao, J.; Lu, Z.; Liao, J.; Zheng, Q.; Huang, F.; Zhou, J.; and Yan, M. 2025. Mobile-Agent-v3: Fundamental Agents for GUI Automation. arXiv:2508.15144.

Zhang, C.; Yang, Z.; Liu, J.; Han, Y.; Chen, X.; Huang, Z.; Fu, B.; and Yu, G. 2023. AppAgent: Multimodal Agents as Smartphone Users. arXiv:2312.13771.

Zheng, B.; Gou, B.; Kil, J.; Sun, H.; and Su, Y. 2024. GPT-4V(ision) is a Generalist Web Agent, if Grounded. arXiv:2401.01614.

Zheng, Y.; Liu, Z.; Zhao, X.; and Wen, J.-R. 2026. A Task-State Representation for Long-Horizon Mobile GUI Agents. *arXiv preprint arXiv:2607.00502*.

Zhou, H.; Wan, X.; Sun, R.; Palangi, H.; Iqbal, S.; Vulicć, I.; Korhonen, A.; and k, S. O. A. 2025. Multi-Agent Design: Optimizing Agents with Better Prompts and Topologies. arXiv:2502.02533.